Numerical Heat Transfer, Part A, 43: 47–64, 2003

1040-7782/03 $12.00 + .00
DOI: 10.1080/10407780390122565

Taylor & Francis
Taylor & Francis Group

PRESSURE DROP AND HEAT TRANSFER IN SPANWISE-PERIODIC FLUTED CHANNELS

Takahiro Adachi
Department of Mechanical Engineering, Akita University, Akita, Japan

Haruo Uehara
President, Saga University, Saga, Japan

We have conducted numerical studies on the three-dimensional laminar forced convection heat transfer in a channel with spanwise-periodic fluted parts by applying the spectral element and finite difference methods. The flow field is assumed to be fully developed, while the temperature field is supposed to be developing under the fully developed velocity profile. The temperature on the plate surface is kept constant. Pressure drop, heat transfer, and correlation between them are investigated for varying configurations of the fluted channel. The nondimensional formulas with regard to the pressure drop and Nusselt number are derived for the parameters of the channel configurations. Channel efficiency, which is defined as the ratio of the heat transfer enhancement to the increase of pressure drop compared with the parallel plate channel, is studied according to the nondimensional formulas to clarify the optimum parameter range of channel configurations.

INTRODUCTION

Improving heat transfer in a heat exchanger is a top priority for many industries. A plate-type heat exchanger currently is widely used, where increasing demand for smaller space and lower noise level tends to make representative size and velocity smaller; thus the Reynolds number becomes smaller. Consequently, it is important to enhance the heat transfer in the laminar flow regime.

We consider a two-phase-type heat exchanger, which must deal with two kinds of working fluids. One such fluid like water is drained into the lower temperature side, while the other, such as steam from evaporating water or chlorofluocarbon, is passed to the higher temperature side. The working fluids used for the lower temperature side are generally in a single-phase state, while those for the higher temperature side are in two-phase state due to condensation.

Received 10 August 2001; accepted 19 April 2002.

We express our thanks to Professor Y. Ikegami, Institute of Ocean Energy, Saga University (IOES), and Ms. N. Visakha for their advice, and Ms. A. Ide, secretary at Saga University, for her encouragement. We also thank Mr. A. Otsuka for helpful comments.

Address correspondence to Takahiro Adachi, Department of Mechanical Engineering, Akita University, Tegata-Gakuen, Akita 010-8502, Japan. E-mail: adachi@ipc.akita-u.ac.jp

NOMENCLATURE

a	height of the fluted part from the centerline
D_h^*	hydraulic diameter $4h^*$
h^*	half height of the parallel plane channel
L^*	half period of the module
l^*	half width of the fluted part
Nu	local Nusselt number
Nu_m	mean Nusselt number
n	distance normal to the wall
Pr	Prandtl number
P, p	pressure
Re	Reynolds number
s	distance along the fluted wall
Θ	nondimensional temperature
Θ_b	local bulk temperature
Θ_i	temperature at inlet
Θ_w	wall temperature
U_0^*	velocity at the origin O, representative velocity
$\mathbf{x}$	coordinate, $\mathbf{x} = (x, y, z)$
x, y, z	components of rectangular coordinate, respectively
$\mathbf{u}$	velocity, $\mathbf{u} = (u, v, w)$
u, v, w	velocity components in x-, y-, and z-, directions, respectively
α^*	heat transfer coefficient
Δp	pressure drop
η	efficiency defined as the ratio of heat transfer enhancement to increase of pressure drop
κ^*	thermal diffusivity
λ^*	thermal conductivity
ν^*	kinematic viscosity
ρ^*	density

Subscripts

c	critical
p	parallel plate channel

Superscript

*	dimensional value

In laminar film condensation with phase changes, plate surfaces with fluted parts along the streamwise direction have been studied particularly for a model of plate-type heat exchanges. The guiding principle for enhancement of heat transfer efficiency is to spread the liquid film as thinly as possible over the widest possible condensing heat transfer surface. Heat transfer is enhanced over an additional area by attaching flutes on its plate surface. This is because strong surface tension aids in the removal of condensate from the top to the bottom of the fluted part, thereby producing a very thin liquid film. In addition to this effect, the liquid layers on the side surfaces of the fins are also expected to become locally very thin when the action of surface tension to bring the liquid into grooves between the fins is strong enough. The effect of surface tension on condensation on a fluted surface was first analysed by Gregorig [1], where the boundary layer theory is applicable because the liquid film is very thin. Later, Kedzierski and Webb [2] extended the analysis of Gregoing to study the practical fin shapes.

On the other hand, little research was done on the single-phase heat transfer in a channel with fluted parts in the streamwise direction because the flow and temperature fields become fully three dimensional, and it is too complicated to analyze them. Sparrow and Charmchi [3] simplified the problem and replaced it with two-dimensional fully developed flow and temperature fields, and analyzed the heat transfer characteristics of a flat channel with a spanwise-periodic corrugated wall. The channel extends infinitely in the spanwise direction. The boundary condition of uniform heat flux was imposed on the corrugated wall, while the flat wall was treated as adiabatic. Sparrow and Chukaev [4] investigated in the same manner the fully developed fluid flow and heat transfer characteristics of a flat channel with spanwise-periodic rectangular corrugations at one wall. Two thermal problems were solved

numerically by successively applying the boundary condition of uniform heat flux at each wall while keeping the other wall adiabatic. Therefore, they did not deal with the three-dimensional problem such as the thermal entrance region. A comprehensive survey of the literature pertinent to the heat transfer behavior and friction loss in fully developed regions has been provided by Shah and London [5] and Kakac et al. [6].

In this paper, we study accurately the problem of single-phase convective heat transfer in a fluted channel under the fully developed flow and developing temperature fields using the spectral element and finite difference methods. The fluted parts are rectangular and are set up spanwise periodically and symmetrically with the midplane of the plates. The temperature on the fluted plate surface is assumed to be constant. Pressure drop, heat transfer, and correlations between them under varying channel geometries are reported, so that the efficient channel configuration with fluted parts can be established numerically.

MATHEMATICAL FORMULATION

We consider a parallel plate channel with spanwise-periodic fluted parts as shown in Figure 1*a*. The figure depicts the channel cross section and indicates the geometric quantities that define its shape. Namely, the channel consists of parallel plates of height $2h^*$ and symmetric fluted part of width $2l^*$ and height a^* measured from the midplane, and the spanwise period is $2L^*$. In view of the symmetries inherent in the spanwise periodic geometry and midplane, we will pay attention only to the typical cross-sectional module OABCDEFG shown in Figure 1*b*.

Take the rectangular coordinate $\mathbf{x} = (x, y, z)$ with the x-axis along the midplane of the parallel plate channel without the flute and the y- and z-axes each perpendicular to it with the origin O as shown in Figure 1. The flow is assumed to be incompressible. The fluid properties are assumed to be constant, and body force effects such as gravity are ignored. The velocity $\mathbf{u}$, the pressure p, and the temperature Θ of the flow are governed by the continuity, Navier–Stokes, and energy equations as

$$\nabla \cdot \mathbf{u} = 0 \tag{1}$$

$$\frac{\partial \mathbf{u}}{\partial t} + (\mathbf{u} \cdot \nabla)\mathbf{u} = -\nabla p + \frac{1}{\mathrm{Re}} \nabla^2 \mathbf{u} \tag{2}$$

$$\frac{\partial \Theta}{\partial t} + (\mathbf{u} \cdot \nabla)\Theta = \frac{1}{\mathrm{Re}\,\mathrm{Pr}} \nabla^2 \Theta \tag{3}$$

where all variables have been nondimensionalized using a characteristic length h^*, velocity U_0^* on the x^*-axis, and temperature Θ_i^* and Θ_w^* as

$$t = \frac{t^* U_0^*}{h^*} \quad \mathbf{x} = \frac{\mathbf{x}^*}{h^*} \quad \mathbf{u} = \frac{\mathbf{u}^*}{U_0^*} \quad p = \frac{p^*}{\rho^* U_0^{*2}} \quad \Theta = \frac{\Theta^* - \Theta_w^*}{\Theta_i^* - \Theta_w^*} \tag{4}$$

where we represent physical quantities with their dimensions by attaching a superscript * to them. The Reynolds number and the Prandtl number in the equations are

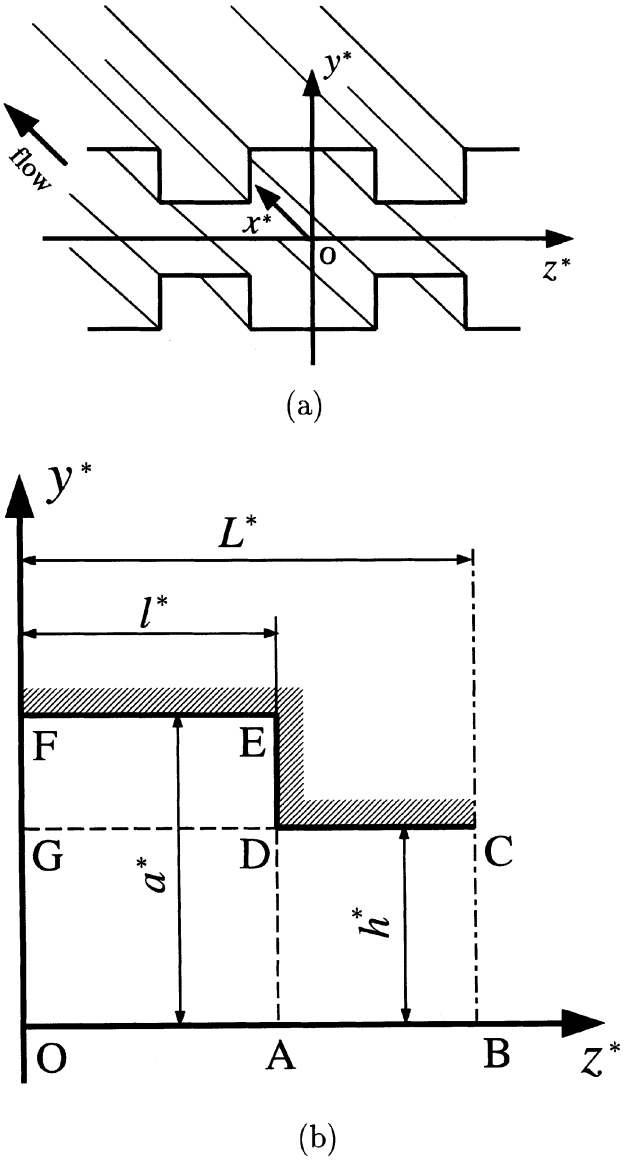

Figure 1. Geometries and coordinates: (*a*) whole geometry, (*b*) calculation domain that is a quarter of the whole geometry.

defined as

$$\mathrm{Re} = \frac{U_0^* h^*}{\nu^*} \qquad \mathrm{Pr} = \frac{\nu^*}{\kappa^*}, \tag{5}$$

where ν^* and κ^* are the kinematic viscosity and the thermal diffusivity of the fluid, respectively.

Moreover, nondimensional parameters to characterize the channel configuration, half period L of the channel, half width l of the fluted part, and height a of the fluted part from the midplane are defined as

$$L = L^*/h^* \quad l = l^*/h^* \quad a = a^*/h^* \tag{6}$$

The channel consists of parallel plates without flute for $a = 1$, whereas it has fluted parts for $a \neq 1$.

Hereafter we are concerned with the problem of the fully developed velocity and developing thermal fields. First we consider a stationary fully developed flow. If we assume the stationary laminar flow in the fluted channel is parallel to the x-axis and unchanged in the axial direction, the velocity $\mathbf{u}$ and the pressure p are expressed as

$$\mathbf{u}(\mathbf{x}, t) = (U(y, z), 0, 0) \tag{7}$$

$$p(\mathbf{x}, t) = P(\mathbf{x}) \tag{8}$$

Substituting Eqs. (7) and (8) into Eqs. (1) and (2), we find that Eq. (1) is automatically satisfied and Eq. (2) is reduced to the following equations:

$$\frac{\partial P}{\partial x} = -\beta = \text{ const.} \tag{9}$$

$$\frac{\partial P}{\partial y} = \frac{\partial P}{\partial z} = 0 \tag{10}$$

$$\left(\frac{\partial^2}{\partial y^2} + \frac{\partial^2}{\partial z^2}\right) U(y, z) = -\beta \,\mathrm{Re} \tag{11}$$

where β is a positive constant representing the pressure gradient downstream.

The boundary condition on the plate surface is given by

$$U(y, z) = 0 \quad \text{at CDEF} \tag{12}$$

In addition to this, the flow is assumed to be symmetric along the lines OAB, BC, and FGO. Then the symmetry boundary conditions are expressed as

$$\frac{\partial U(y, z)}{\partial y} = 0 \quad \text{at OAB} \tag{13}$$

$$\frac{\partial U(y, z)}{\partial z} = 0 \quad \text{at BC and FGO} \tag{14}$$

Second, we consider thermally developing field under the fully developed velocity profile. We presume negligible axial heat conduction when RePr is large enough, and the wall temperature and temperature of the fluid at the inlet of the channel are constant. Then Eq. (3) is reduced to the following form:

$$U(y,z)\frac{\partial\Theta(x,y,z)}{\partial x}=\frac{1}{\mathrm{Re}\,\mathrm{Pr}}\left(\frac{\partial^2}{\partial y^2}+\frac{\partial^2}{\partial z^2}\right)\Theta(x,y,z) \tag{15}$$

where x is taken from the thermal entrance point and the velocity profile is fully developed at $x=0$. This gives an extended version of the Graetz–Nusselt problem [7].

The boundary condition at the thermal entrance point is given by

$$\Theta(x,y,z)=1 \quad \text{at } x=0 \tag{16}$$

On the other hand, the boundary condition on the plate surface is given by

$$\Theta(x,y,z)=0 \quad \text{at CDEF} \tag{17}$$

Also for the temperature field, the symmetry boundary conditions are imposed at OAB, BC, and FGO as

$$\frac{\partial\Theta(x,y,z)}{\partial y}=0 \quad \text{at OAB} \tag{18}$$

$$\frac{\partial\Theta(x,y,z)}{\partial z}=0 \quad \text{at BC and FGO} \tag{19}$$

NUMERICAL METHOD

To calculate the fully developed flow, we obtain the velocity distribution $U(y,z)$ of the stationary flow by solving a two-dimensional potential equation (11) under the boundary conditions given by Eqs. (12)–(14). As the linearity of the boundary value problem tells us at a glance, the magnitude of the solution $U(y,z)$ is proportional to $\beta\,\mathrm{Re}$. Therefore, if a solution is obtained for a certain value of $(\beta\,\mathrm{Re})_0$, the solution for an arbitrary value of $\beta\,\mathrm{Re}$ is immediately derived from it. Normalizing $U(0,0)=1$, which means that the solution is divided by $U(0,0)$ for $(\beta\,\mathrm{Re})_0$ and then the right-hand side of Eq. (11) becomes $(\beta\,\mathrm{Re})_0/\{U(0,0)$ for $(\beta\,\mathrm{Re})_0\}$ (refer to Tatsumi and Yoshimura [12]), we can obtain the solution that is equivalent to adopting the dimensional velocity on the origin O as the characteristic velocity. To calculate the developing thermal field, substituting the resulting $U(y,z)$ into Eq. (15), we obtain the temperature field in the thermal entrance region under the fully developed flow.

The numerical calculations are carried out by utilizing the spectral element method [8, 9] in (y,z) components with the finite difference method in the x-direction. In the spectral element method, the actual solution domain is broken up into three elements in this study (OADG, ABCD, and DEFG in Figure 1*b*), and each element is mapped from the physical (y,z) space to the local $(\bar{y},\bar{z})$) coordinate system whose ranges are $[-1, 1]$, respectively. The velocity and temperature are expanded by high-order Lagrangian interpolants through Gauss–Lobatto Chebyshev collocation points, defined as

$$U^k(\bar{y},\bar{z}) = \sum_{m=0}^{N}\sum_{n=0}^{N} U^k_{mn} h_m(\bar{y}) h_n(\bar{z}) \qquad (k = 1,2,3) \tag{20}$$

$$\Theta^k(x,\bar{y},\bar{z}) = \sum_{m=0}^{N}\sum_{n=0}^{N} \Theta^k_{mn}(x) h_m(\bar{y}) h_n(\bar{z}) \qquad (k = 1,2,3) \tag{21}$$

where the interpolants are expressed as

$$h_i(\bar{\zeta}) = \frac{2}{N}\sum_{n=0}^{N}{}'' \frac{1}{c_j c_n} T_n(\bar{\zeta}_j) T_n(\bar{\zeta}) \tag{22}$$

$$c_l = 1 \qquad l \neq 0, N \tag{23}$$

$$c_l = 2 \qquad l = 0, N \tag{24}$$

where the T_n are the nth order Chebyshev polynomials and $i = m,n$ and $\bar{\zeta} = \bar{y}, \bar{z}$. The Gauss–Lobatto points are defined as

$$\bar{\zeta}_j = \cos\frac{\pi j}{N} \qquad j = 0, 1, \ldots, N \tag{25}$$

Substituting the expansions of Eqs. (20) and (21) into the weak forms of Eqs. (11) and (15) and also using the Galerkin method, we obtain a set of algebraic equations for U^k_{mn} and a set of ordinary differential equations with respect to x for $\Theta^k_{mn}(x)$. The set of equations for $\Theta^k_{mn}(x)$ is solved in the thermal entrance region by the finite difference method with an increment of $\Delta\bar{x}$ where we put $\bar{x} = x/\mathrm{Re}\,\mathrm{Pr}$, and the Crank–Nicholson scheme is used. The fully developed temperature field is determined when the mean Nusselt number on the fluted wall, which is defined at later section, becomes independent of $\bar{x}$ and the maximum relative difference of two successive steps of $\bar{x}$ reaches 10^{-7}. The magnitude of $\Delta\bar{x}$ is taken as $\Delta\bar{x} = 1 \times 10^{-5}$, and truncation parameters are taken as $N = 8$, which are confirmed as being large enough by comparing results for various values of N. For example, the mean Nusselt number for parallel plate channel ($a = 1$, $L = 4$) is 7.5406, which shows within 0.01% a relative error with the analytical value of 7.541 [5].

RESULTS

The numerical calculation has been carried out for the parameter $L = 4$, which is fixed, and for $l = 0.5$ to 3.5 changed by every 0.5 and $a = 1$ to 4 changed by every 0.2.

Flow Field and Pressure Drop

The velocity distributions $U(y,z)$ for $(l,a) = (0.5,2.5)$, (1.0,2.0), and (1.5,1.5) are depicted in Figure 2 as typical examples. The isovelocity contour levels have been chosen to be at 0.05 intervals. It is seen that the velocity is maximum in the center of

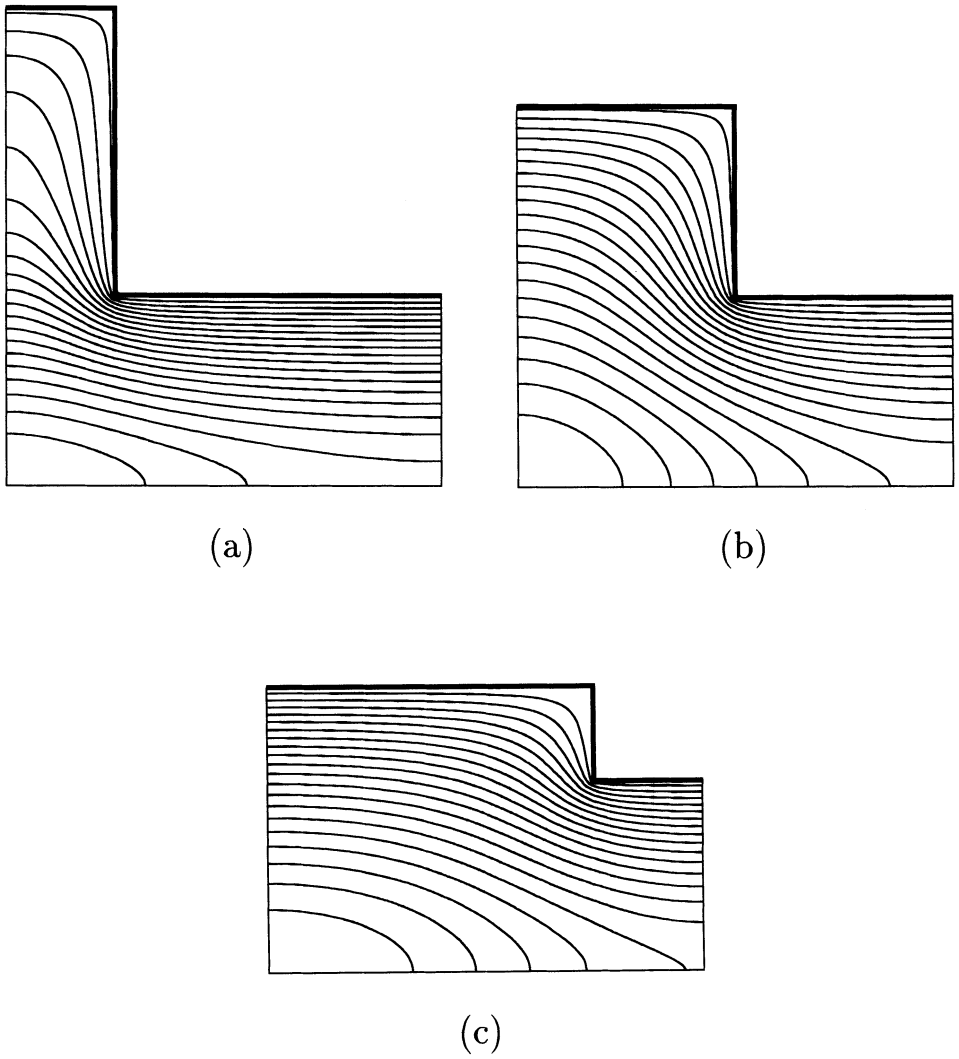

Figure 2. Fully developed flow field of U: (*a*) $l=0.5$ and $a=2.5$, (*b*) $l=1.0$ and $a=2.0$, (*c*) $l=1.5$ and $a=1.5$.

the channel, and it becomes smaller near the plate surface. The fluted part becomes taller as a increases and l decreases, so that the contour lines of U are sparse inside the fluted part. Then we find that the velocity gradient becomes slower especially in the portion of an edge.

We consider the effect of flute on the pressure drop. Now we define the quantity $\Delta P/\Delta P_p$ as a ratio of the pressure gradient for the fluted channel to the corresponding quantity for a parallel plate channel with height $2h^*$, which corresponds to the friction coefficient ratio, defined as

$$\frac{\Delta P}{\Delta P_p} = \frac{1}{2}\left(\frac{(\beta\,\mathrm{Re})_0}{U(0,0)\ \text{for}\ (\beta\,\mathrm{Re})_0}\right) \tag{26}$$

where

$$\Delta P = \frac{\mathrm{d}P}{\mathrm{d}x}\left(\frac{(\beta\,\mathrm{Re})_0}{U(0,0)\ \text{for}\ (\beta\,\mathrm{Re})_0}\right)\frac{1}{\mathrm{Re}} \tag{27}$$

from Eqs. (9) and (11), and $\Delta P_p = 2/\mathrm{Re}$ from the velocity profile of plane Poiseuille flow. It is found that Eq. (26) is independent of the Reynolds number.

In Figure 3*a*, we plot $\Delta P/\Delta P_p$ for each l against a. It is clear that $\Delta P/\Delta P_p$ is always less than unity, thus showing that the effect of the addition of a flute to a parallel plate channel is one of drag reduction. This is due to stress relaxation at the boundary line between the main flow and the fluted part as well as due to stress reduction along the fluted wall surface from the smaller velocity gradient. As shown in Figure 3*a*, $\Delta P/\Delta P_p$ decreases and converges asymptotically to a constant value for each l as a increases. On the other hand, it tends to unity as l decreases because the channel approaches the parallel plate channel.

For practical applications, it is desirable to derive a nondimensional formula that shows the relationship between the pressure drop ratio and the geometric parameters of the channels. The pressure drop ratios are correlated with the least square curve fitting method for the geometric parameters l and a, and the following equation is obtained as

$$\frac{\Delta P}{\Delta P_p} = \exp(0.0389 - 0.238 l^{1.5}) + \frac{l^2 a^{-1.96-3.26/l^{1.5}}}{4.78 + 0.905 l^2} \tag{28}$$

As shown in Figure 3*b*, the pressure drop ratio obtained by the formula deviates by less than 2% from the value given by the numerical calculation, where the vertical axis shows the result obtained by the numerical calculation, and the horizontal one indicates the value of the approximation formula for the given geometric parameters a and l.

Thermal Field and Heat Transfer

The temperature distributions $\Theta(x, y, z)$ in the thermal entrance region for $(l, a) = (0.5, 2.5)$, (1.0, 2.0), and (1.5, 1.5) are depicted in Figure 4, which illustrates three dimensionally the evolution of temperature fields from $x/\mathrm{Re}\,\mathrm{Pr} = 0$ to 2. The thermal boundary layer builds up along the plate surface, accelerating the heat transfer in the otherwise undisturbed core. Note that the temperature distribution for the fluted parts are more developed than that for the plate without the flute. It eventually occupies the entire region and defines a fully developed temperature field. The fully developed temperature distributions $\Theta(x, y, z)$ for $(l, a) = (0.5, 2.5)$, (1.0, 2.0), and (1.5, 1.5) are depicted in Figure 5. It is seen that the temperature is highest in the center of the channel, and it reduces near the plate surface as well as the velocity distribution. It is clear that the contour lines of Θ are sparse inside the

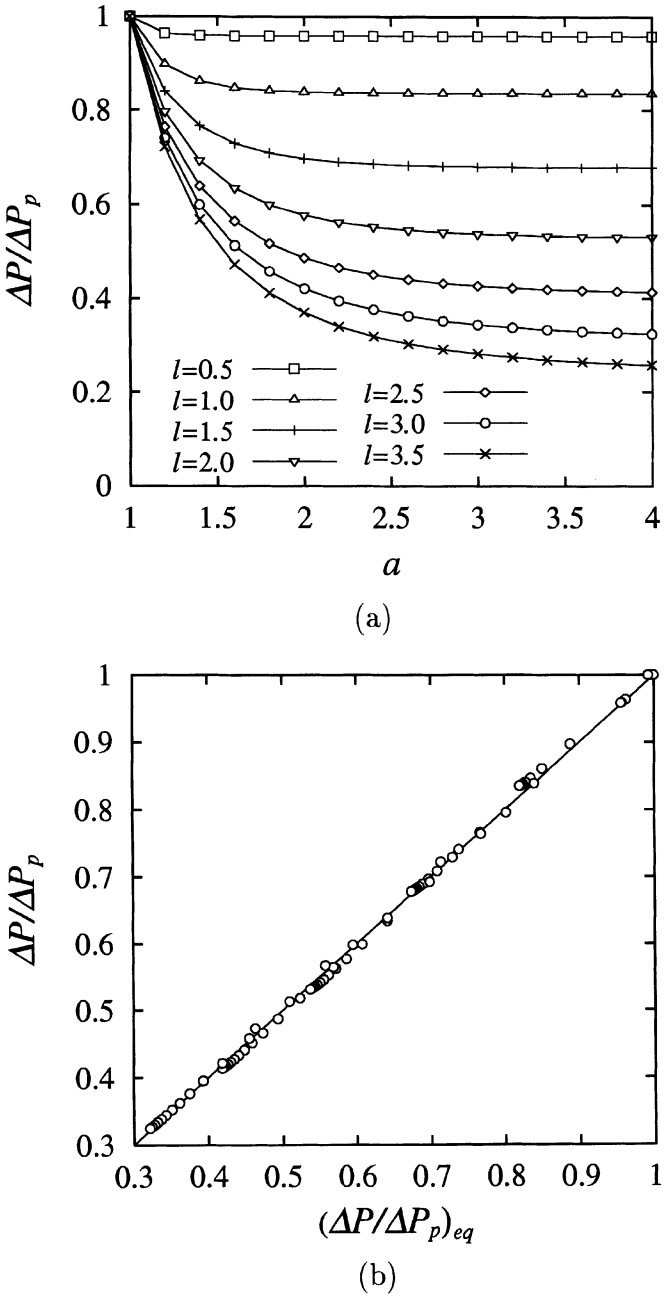

Figure 3. Pressure drop ratio: (*a*) $\Delta P/\Delta P_p$ for each l against a, (*b*) comparison with $\Delta P/\Delta P_p$ of numerical calculation and $(\Delta P/\Delta P_p)_{eq}$ of the nondimensional formula.

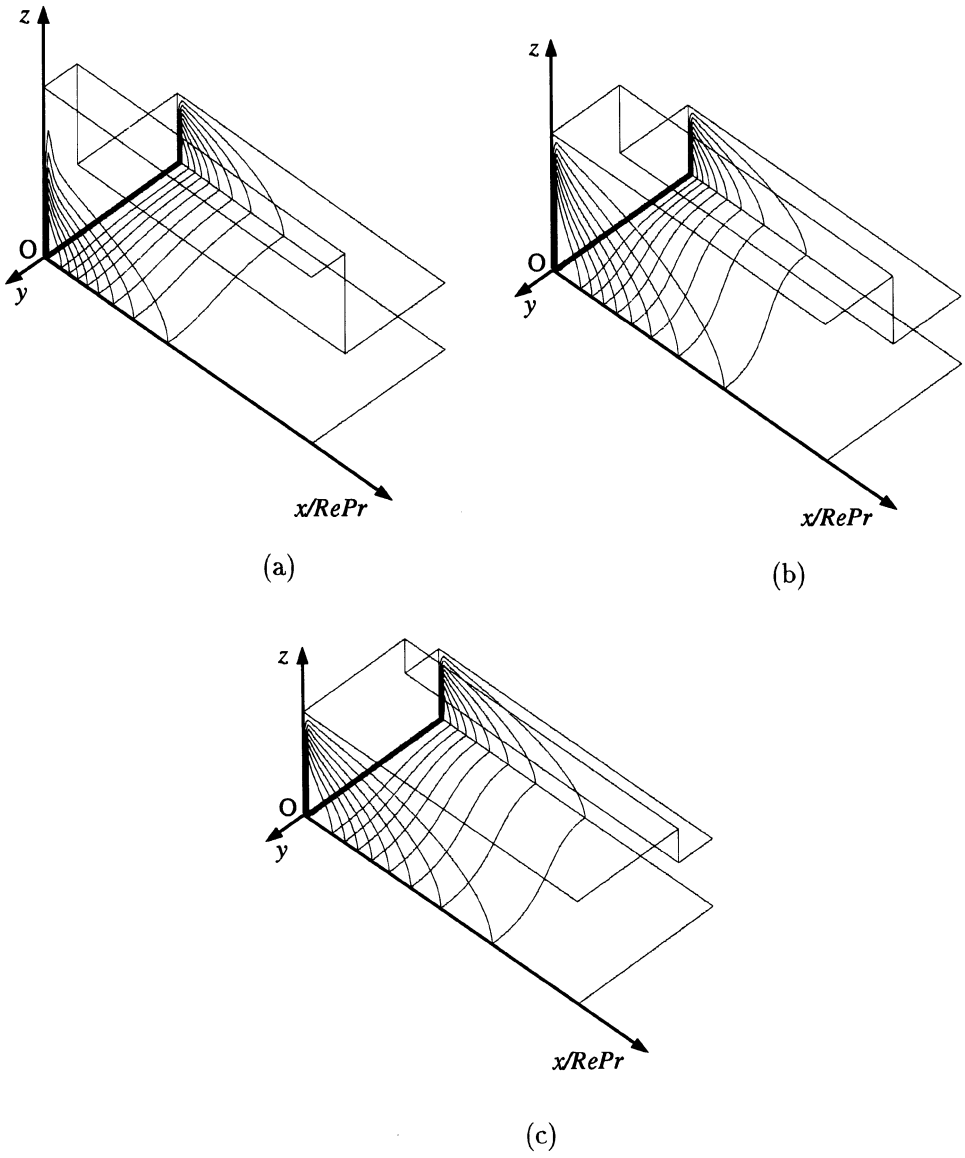

Figure 4. Three-dimensional development of the temperature field in thermal entrance region. $0 \leq x/\mathrm{Re}\,\mathrm{Pr} \leq 2$: (*a*) $l = 0.5$ and $a = 2.5$, (*b*) $l = 1.0$ and $a = 2.0$, (*c*) $l = 1.5$ and $a = 1.5$.

fluted part as a increases and l decreases, which may lead to reduction of heat transfer particularly in the portion of an edge.

Next we consider the effect of flute on the heat transfer. A local Nusselt number, Nu, is defined as

$$\mathrm{Nu}(s) = \frac{\alpha^* D_h^*}{\lambda^*} = \frac{4}{\Theta_w - \Theta_b}\left(\frac{\partial \Theta}{\partial n}\right)_{w,s} \tag{29}$$

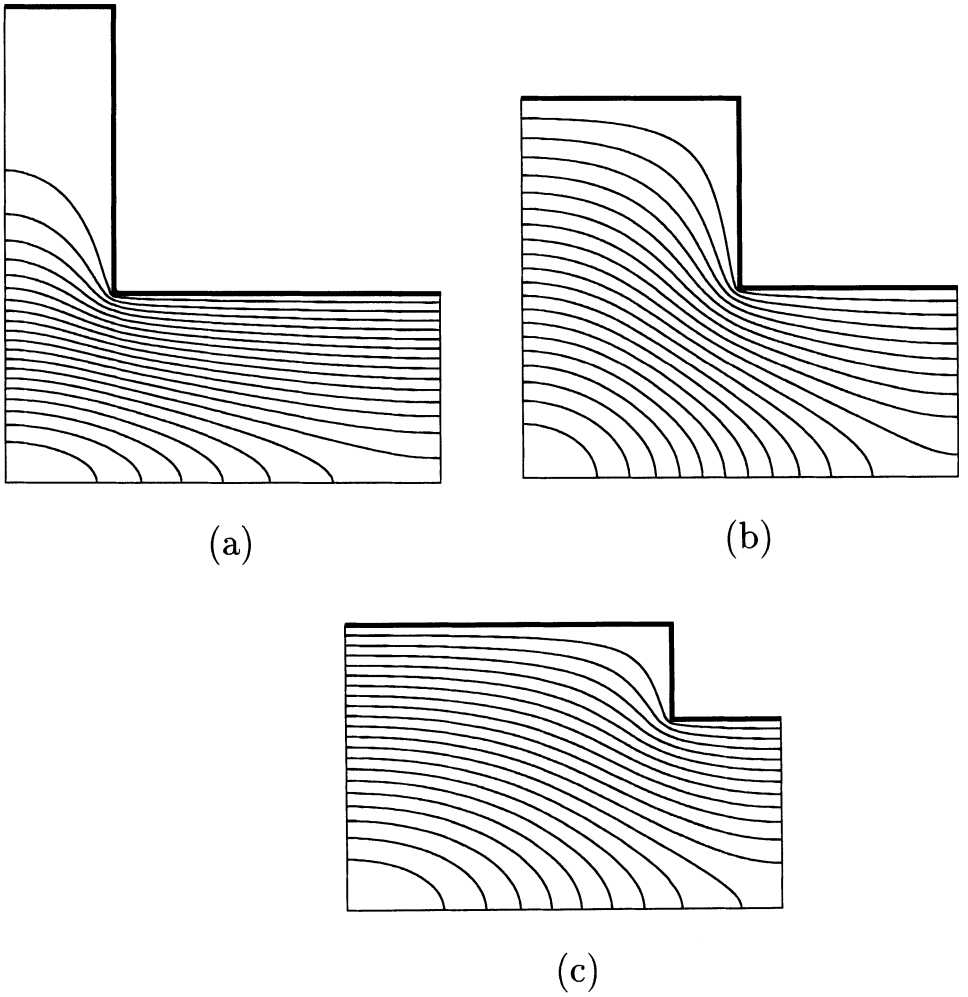

Figure 5. Fully developed temperature field: (*a*) $l=0.5$ and $a=2.5$, (*b*) $l=1.0$ and $a=2.0$, (*c*) $l=1.5$ and $a=1.5$.

where α^* is the heat transfer coefficient, λ^* is the thermal conductivity of the fluid, $D_h^*(=4h^*)$ is the hydraulic diameter and the constant, $(\partial\Theta/\partial n)_{w,s}$ is the temperature gradient normal to the wall at the position s along the channel wall, and $\Theta_b(x)$ is the cross-sectional local bulk temperature defined as

$$\Theta_b(x) = \frac{\int\int \Theta(x,y,z)U(y,z)dy\,dz}{\int\int U(x,y,z)dy\,dz} \tag{30}$$

The integrals are to be carried over the cross-sectional area of the channel. The mean Nusselt number Nu_m is defined as

$$\mathrm{Nu}_m = \frac{1}{L+(a-1)}\int_0^{L+(a-1)} \mathrm{Nu}(s)ds \tag{31}$$

We define the quantity $\mathrm{Nu}_m/\mathrm{Nu}_p$ to be the ratio of the mean Nusselt number for the fluted channel to the corresponding quantity for parallel plate channel with height $2h^*$ and $\mathrm{Nu}_p = 7.54$ [5]. In Figure 6, $\mathrm{Nu}_m/\mathrm{Nu}_p$ of the entrance region is depicted for three typical cases. The Nusselt number ratio changes from a thermal entrance along the direction of the x-axis, as shown in the figure. It is clear that $\mathrm{Nu}_m/\mathrm{Nu}_p$ is greater than unity for $x/\mathrm{Re}\,\mathrm{Pr} < 0.02$, and after that it reduces to less than unity due to a decrease of heat transfer to the plate surface in the fluted part compared with that of the parallel plate channel. The effect of the addition of a flute to the parallel plate channel is thought to be one of heat maintenance. If the distance from the thermal entrance exceeds $x/\mathrm{Re}\,\mathrm{Pr} \sim 0.3$, the Nusselt number ratios mostly converge on the constant values. Therefore, we can see that the temperature field is in the fully developed state for $x/\mathrm{Re}\,\mathrm{Pr} > 0.3$, and then $x/\mathrm{Re}\,\mathrm{Pr} \sim 0.3$ gives the length of the thermal entrance region, where the velocity profile is fully developed at $x = 0$. Furthermore, we have confirmed that these results are also the same with the cases of the other geometric parameters studied here.

The ratio $\mathrm{Nu}_m/\mathrm{Nu}_p$ in a fully developed temperature field is plotted against a for each l in Figure 7*a*. It turns out that we obtain two different kinds of tendency as shown in Figure 7*a*, depending on the magnitude of l, large or small. Namely, for the case of $l \leq 1.5$, $\mathrm{Nu}_m/\mathrm{Nu}_p$ decreases monotonically as a increases. On the other hand, for the case of $l \geq 2.0$, it decreases and converges asymptotically on constant values as a increases.

For each case such as $l \leq 1.5$ or $l \geq 2.0$, the Nusselt number ratio is correlated to the least square curve fitting method for the geometric parameters l and a, and the following equations are obtained, respectively, as

$$\frac{\mathrm{Nu}_m}{\mathrm{Nu}_p} = 0.821 - 1.93\ \exp(-l) + \{0.163 + 1.94\ \exp(-l)\}a^{-0.385-0.329l^3} \quad \text{for } 0.5 \leq l \leq 1.5 \tag{32}$$

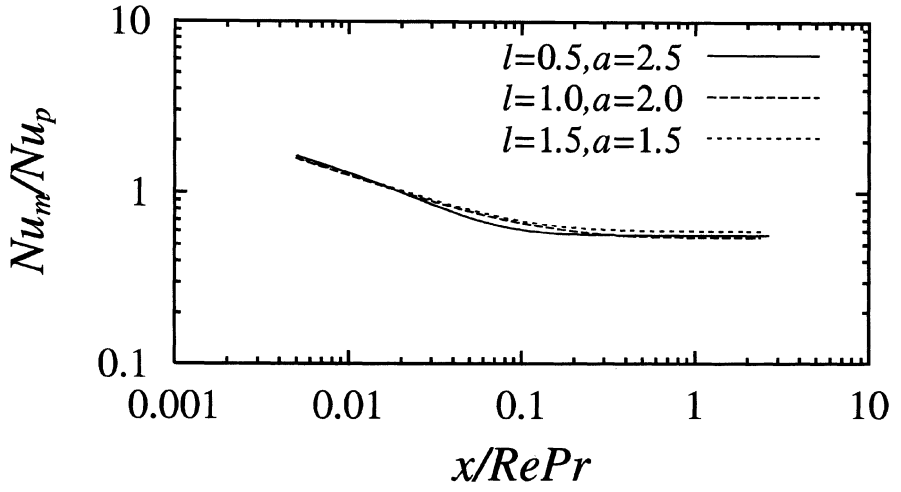

Figure 6. Evolution of Nusselt number ratio along $x/\mathrm{Re}\,\mathrm{Pr}$.

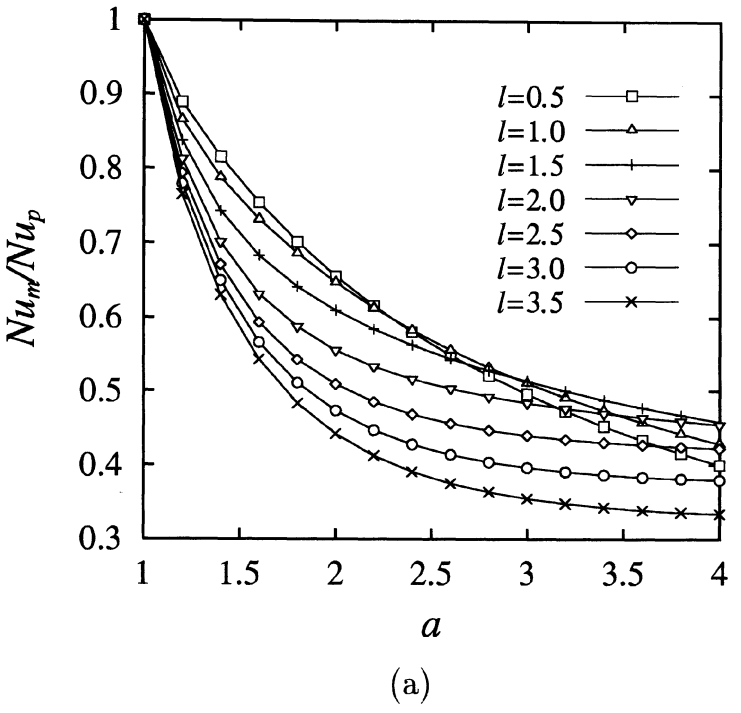

Figure 7*a*. Nusselt number ratio: (*a*) $\mathrm{Nu}_m/\mathrm{Nu}_p$ for each l against a.

$$\frac{\mathrm{Nu}_m}{\mathrm{Nu}_p} = 0.496 - 0.0162l^2 + (0.504 + 0.0165l^2)a^{1.28-9.98\ \ln(l)/l} \quad \text{for } 2.0 \le l \le 3.5 \tag{33}$$

As shown in Figures 7*b* and 7*c*, the Nusselt number ratio obtained by the formulas deviates less than 2% from the value given by the numerical calculation, where the vertical axis shows the result obtained by numerical calculation, and the horizontal one shows the value of the approximation formulas for the given geometric parameters l and a.

Correlation Between Pressure Drop and Heat Transfer

It is vitally important to know the channel configuration to improve efficiency, which will be decided by correlative factors between heat transfer and pressure drop. We define a channel efficiency η as the ratio of the heat transfer enhancement to the increase of pressure drop compared with the parallel plate channel as

$$\eta = \frac{\mathrm{Nu}_m/\mathrm{Nu}_p}{\Delta P/\Delta P_p} \tag{34}$$

where Eqs. (28), (32), and (33) are used for the pressure drop and Nusselt number ratios, which show the correlation between heat transfer and pumping power.

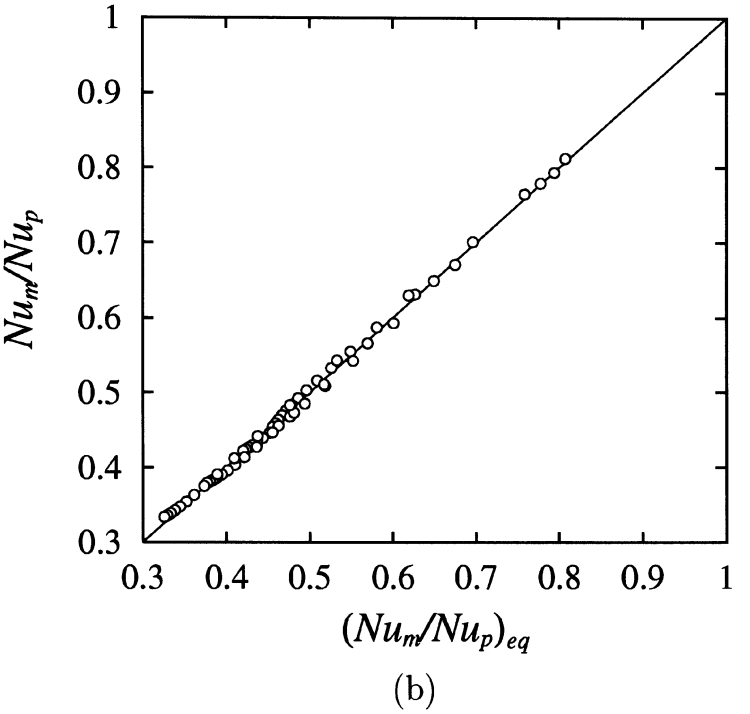

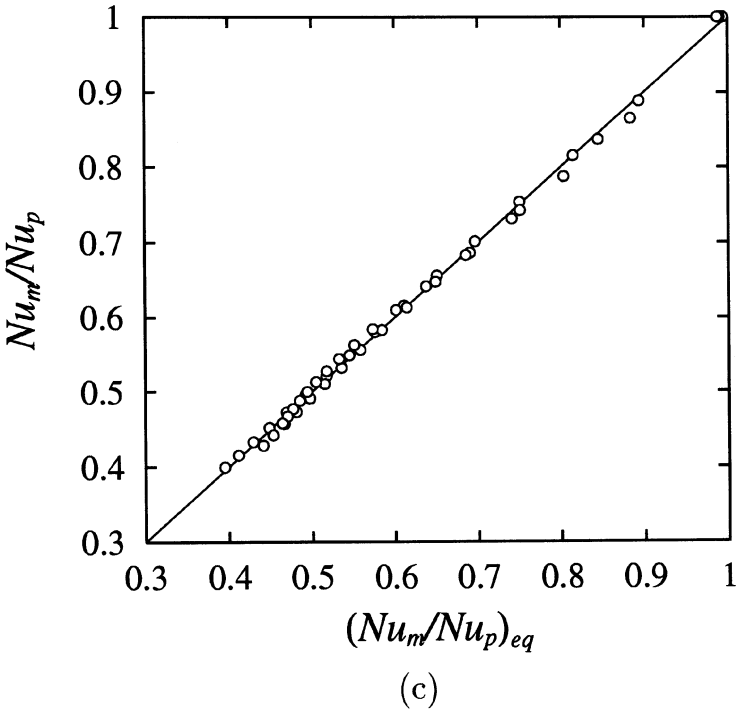

Figure 7*b–c*. Nusselt number ratio: (*b*) comparison with Nu_m/Nu_p of numerical calculation and $(Nu_m/Nu_p)_{eq}$ of the nondimensional formula for $0.5 \leq l \leq 1.5$, (*c*) comparison with Nu_m/Nu_p of numerical calculation and $(Nu_m/Nu_p)_{eq}$ of the nondimensional formula for $2.0 \leq l \leq 3.5$.

In Figure 8, we show the contour lines of η against a and l in a bit larger range than that which is ordinarily applied for each formula of the Nusselt number ratio. In these figures, the region $\eta > 1$ means that the heat transfer enhancement exceeds the increase of pressure drop, and the efficiency of the fluted channel is superior to the parallel plate one. The region $\eta > 1$ is indicated by solid lines, while the region $\eta < 1$ by dashed lines. In Figure 8*a*, η exceeds unity in the near range of $l > 1$ and becomes larger as a and l become larger, with the maximum value of $\eta = 4.21$ at $(a, l) = (4, 2)$, although the values of the parameter are out of the limit of Eq. (32). On the other hand, in Figure 8*b*, η exceeds unity in the near range of $l < 2.75$ and has a maximum value of $\eta = 1.52$ at $(a, l) = (4, 2.2)$. Therefore, it is evident that the optimum parameter ranges as η exceeds unity are roughly $1 < l < 2.75$ independent of a.

The pressure loss and heat transfer in the steady laminar flow state have been dealt with here. Generally, if the Reynolds number becomes larger and goes through a certain critical value, the flow bifurcates to an unsteady flow state. For example, the critical Reynolds number of the flow in the parallel plate channel without flute is $\mathrm{Re}_c = 5772$ by the linear stability analysis [10], or $\mathrm{Re}_c = 4350$ by the nonlinear stability one [11]. The critical value, however, is not clear for the flow in the fluted channel because, using the three-dimensional stability analysis, it is too difficult to obtain the critical value as shown by Tatsumi and Yoshimura [12] who carried out the stability analysis for a rectangular duct flow without flute. The stability of flow in spanwise-periodic fluted channels is for future study.

On the other hand, if the flow becomes unsteady in a channel with streamwise-periodic eddy promoters, it leads to the enhancement of heat transfer and increase in pressure drop due to flow mixing and periodic interruptions of thermal boundary layers, as already clearly explained by Adachi and Uehara [13, 14], Wirtz et al. [15], and Greiner et al. [16]. Especially the efficiency of channels with rectangular eddy promoters exceeds unity once the flow becomes unsteady, although η is less than unity for the steady flow [14]. In this study, however, it should be noted that the enhancement of heat transfer to the parallel plate channel has shown exceeding increase of pressure loss to the parallel plate one even in the steady laminar state. This fact is useful for studying heat transfer enhancement and reduction of pressure loss, particularly in a low Reynolds number regime.

CONCLUDING REMARKS

We have performed a numerical investigation for the flow and temperature fields in a channel with spanwise-periodic fluted parts as a simple model of a plate-type heat exchanger. Numerical calculations of three-dimensional fully developed flow and developing temperature fields have been carried out by using the spectral element and finite difference methods for the channel configurations $L = 4$, which is fixed, and for $l = 0.5$ to 3.5 changed by every 0.5 and $a = 1$ to 4 changed by every 0.2.

The main conclusions are summarized as follows:

1. We have derived nondimensional formula (Eq. (28)), which expresses the relationship between the ratio of the pressure drop of the fluted channels and that of the parallel plate channels and geometric parameters of the fluted channels.

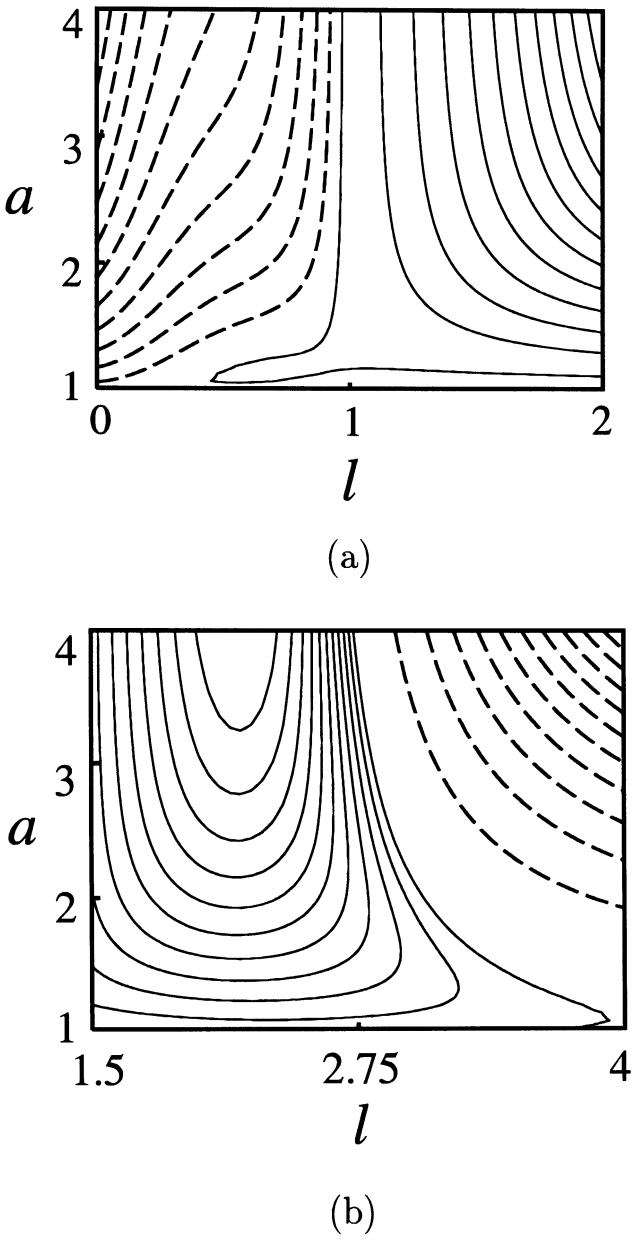

Figure 8. Contours of channel efficiency against the geometric parameters: (*a*) $0 < l < 2$, (*b*) $1.5 < l < 4$.

2. We have obtained information about the length of the thermal entrance region, three-dimensional temperature distribution, and development of Nusselt number in the thermally developing region.
3. We have derived the nondimensional formulae (Eqs. (33) and (32)), which express the relationship between the ratio of the mean Nusselt number of

the fluted channels to that of the parallel plate channels and geometric parameters of the fluted channels, for the fully developed temperature field.

4. We have analyzed the channel efficiency from the obtained nondimensional formulas for pressure drop and Nusselt number ratios, and revealed the optimal geometric parameter range of the fluted channels.

REFERENCES

1. R. Gregorig, Hautkondensation an Feingewellten Oberflächen bei Berücksichtigung der Oberflächenspannungen, *Z. Angew. Math. Phys.*, vol. 5, pp. 36–49, 1954.
2. M. A. Kedzierski and R. L. Webb, Practical Fin Shapes for Surface-Tension-Drained Condensation, *ASME J. Heat Trans.*, vol. 112, pp. 479–485, 1990.
3. E. M. Sparrow and M. Charmchi, Heat Transfer and Fluid Flow Characteristics of Spanwise-Periodic Corrugated Ducts, *Int. J. Heat and Mass Trans.*, vol. 23, pp. 471–481, 1980.
4. E. M. Sparrow and A. Chukaev, Forced-Convection Heat Transfer in a Duct Having Spanwise-Periodic Rectangular Perturbances, *Numer. Heat Transfer*, vol. 3, pp. 149–167, 1980.
5. R. K. Shah and A. L. London, Laminar Flow Forced Convection in Ducts, *Adv. Heat Transfer*, Suppl. I, pp. 153–195, 1978.
6. S. Kakac, R. K. Shah, and W. Aung, *Handbook of Single-Phase Convective Heat Transfer*, chap. 17, Wiley-Interscience, New York, 1987.
7. H. D. Baehr and K. Stephan, *Heat and Mass Transfer*, chap. 3, Springer-Verlag, Berlin, Heidelberg, 1998.
8. A. T. Patera, A Spectral Element Method for Fluid Dynamics: Laminar Flow in a Channel Expansion, *J. Compt. Phys.*, vol. 54, pp. 468–488, 1984.
9. G. E. Karnidakis, *Spectral/hp Element Methods for CFD*, chap. 2, Oxford University Press, Oxford, 1999.
10. S. A. Orzsag, Accurate Solution of the Orr-Sommerfeld Stability Equation, *J. Fluid Mech.*, vol. 50, pp. 689–703, 1971.
11. A. Fortin, M. Jardak, J. J. Gervais, and R. Pierre, Old and New Results on the Two-Dimensional Poiseuille Flow, *J. Compt. Phys.*, vol. 115, pp. 455–469, 1994.
12. T. Tatsumi and T. Yoshimura, Stability of the Laminar Flow in a Rectangular Duct, *J. Fluid Mech.*, vol. 212, pp. 437–449, 1990.
13. T. Adachi and H. Uehara, Transitions and Pressure Drop Characteristics of Flow in Channels with Periodically Grooved Parts, *JSME Int Journal Series B*, vol. 44, pp. 221–230, 2001.
14. T. Adachi and H. Uehara, Correlation Between Heat Transfer and Pressure Drop in Channels with Periodically Grooved Parts, *Int. J. Heat and Mass Trans.*, vol. 44, pp. 4333–4343, 2001.
15. R. A. Wirtz, F. Huang, and M. Greiner, Correlation of Fully Developed Heat Transfer and Pressure Drop in a Symmetrically Grooved Channel, *ASME J. Heat Trans.*, vol. 121, pp. 236–239, 1999.
16. M. Greiner, R. J. Faulkner, V. T. Van, H. M. Tufo, and P. F. Fischer, Simulations of Three-Dimensional Flow and Augmented Heat Transfer in a Symmetrically Grooved Channel, *ASME J. Heat Trans.*, vol. 122, pp. 653–660, 2000.